

International Journal of Modern Physics D
 © World Scientific Publishing Company

General relativistic two-temperature accretion solutions for spherical flows around black holes

Shilpa Sarkar

*Aryabhatta Research Institute of Observational Sciences,
 Manora Peak, Nainital, Uttarakhand 263002, India
 shilpa@aries.res.in*

Indranil Chattopadhyay

*Aryabhatta Research Institute of Observational Sciences,
 Manora Peak, Nainital, Uttarakhand 263002, India
 indra@aries.res.in*

Received Day Month Year

Revised Day Month Year

Matter falling onto black holes is hot, fully ionized and has to be necessarily transonic. Since the electrons are responsible for radiative cooling via processes like synchrotron, bremsstrahlung and inverse-Compton, therefore the electron gas and proton gas are supposed to settle into two separate temperature distribution. But the problem with two-temperature flow is that, there is one more variable than the number of equations. Accretion flow in its simplest form is radial, which has two constants of motion. While, the flow variables are, the radial bulk three-velocity, electron and proton temperatures. Therefore, unlike single temperature flow, in the two temperature regime, there are multiple transonic solutions, non-unique for any given set of constants of motion with a large variation in sonic points. We invoked the second law of thermodynamics to find a possible way to break the degeneracy, by showing only one of solutions among all possible, has maximum entropy and therefore is the correct solution. By considering these correct solutions, we showed that the accretion efficiency increase with the increase in the mass accretion rate. We showed that radial flow onto super-massive black hole can radiate with efficiency more than 10%, if the accretion rate is more than 60% of the Eddington accretion rate, but accretion onto stellar-mass black hole achieve the same efficiency, when it is close to the Eddington limit. We also showed that, dissipative heat quantitatively affects the two temperature solution. In presence of explicit heat processes the Coulomb coupling is weak.

Keywords: Accretion – black hole physics –hydrodynamics – radiative process

PACS numbers: 4.70.-s, 47.40.Hg, 51.30.+i, 95.30.Jx, 95.30.Lz, 97.10.Gz

1. Introduction

One of the most spectacular objects found in the Universe are black holes (BH). Although not directly observable, their presence is interpreted from the huge amount of energy they liberate through a process called accretion. BH is an extreme compact

object found, with sizes of the order of $\sim 3\text{km}$ (M_{BH}/M_{\odot}), where M_{BH} is the mass of BH and M_{\odot} is the solar mass. Due to their compactness, the amount of energy released due to accretion might be of the order of the rest mass energy of the matter falling onto it. In the Universe, there exists stellar-mass BHs which accrete matter from a companion star and are visible in the sky as X-ray binaries, or may exist as super-massive ($\sim 10^6 - 10^9 M_{\odot}$) BHs which can feed on a full galaxy. Centres of such active galaxies are famously known as the Active Galactic Nuclei (AGN) and are one of the brightest sources observed in the Universe.

The advent of the theory of accretion onto compact objects began with the seminal works done by Hoyle & Lyttleton (1939)¹ and Bondi (1952)², where they studied radial flow onto a gravitating centre. With the discovery of quasars³ and X-ray sources⁴ in 1960s, accretion of matter onto compact objects gained popularity. That is because, accretion onto a BH is the only plausible mechanism which could explain such high luminosities. In 1964, Salpeter⁵, computed the luminosity by using the Bondi accretion model, but failed to match it with observations. Matter being radially falling in case of Bondi flows, do not get sufficient time to radiate. The general relativistic version of Bondi flow was presented by Michel (1972)⁶ and this version of Bondi flow was also found out to be ‘too fast’ to produce significant radiation⁷. At about the same time, the famous Shakura-Sunyaev disc (SSD) or the Keplerian disc (KD) model was proposed⁸. Since Bondi flow could not explain the observed luminosity, therefore a rotation dominated disc model was envisaged in order to mitigate the effect of very fast infall velocity. KD or SSD model assumes that matter is rotating with Keplerian azimuthal velocity, with an anomalous viscosity removing angular momentum outwards to accrete matter inwards. The heat generated is radiated away efficiently and the spectra produced by the disc is multi-coloured black body. Though this model could explain the thermal component of the spectrum but was unable to explain the high energy, non-thermal part of the spectrum. It was also realized that the flow should not be Keplerian everywhere especially near the BH. Therefore the inner region of an accretion flow has to be sub-Keplerian and has to pass through the sonic point at least once before crossing the horizon as was shown by Liang & Thompson⁹ (hereafter, LT80). Subsequently, there was a significant body of work done by a number of workers on advective, transonic flows. Transonic flow has been studied for inviscid disc, viscous disc, around rotating BHs, discs harbouring shocks and host of other circumstances^{10–23}. While for inviscid, adiabatic flow the sonic point can be obtained by solving a polynomial equation for a given Bernoulli parameter and specific angular momentum, but obtaining sonic points for accretion flow in presence of heating and radiative cooling processes is not trivial. One can arbitrarily change the inner, or outer boundary conditions in order to obtain some solutions, but without a systematic approach it may lead to obtaining limited class of solutions or a few unphysical ones. In that context, Gu & Lu (2004)²⁴ used the generalized Bernoulli parameter which is also a constant of motion to obtain transonic viscous accretion solutions for a particu-

lar viscosity prescription²⁵. The approach of Becker & Le (2003)²⁶ and Becker et al. (2008),²⁷ of using the generalized Bernoulli parameter simultaneously with the measure of entropy close to the horizon, to find the sonic point and therefore the transonic solution, is physically the most correct approach. Based on this approach, many papers were written to obtain solutions in single temperature accretion flows around BHs^{19, 21, 22, 28, 29}. Single temperature solutions are important to the extent that, it gives a general idea about the flow behaviour, its dynamics as well as energetics. To study the luminosity and spectra of the accreting flow, one need to know electron temperature of the flow, which may or may not be same as the proton temperature.

Due to the extreme gravity, matter falling onto a BH is very hot and becomes fully ionized. A fully ionized astrophysical plasma would be mostly composed of electrons and protons because hydrogen is the most abundant element. Electrons radiate most of the energy and protons do not, in addition, the Coulomb coupling time scale is longer than the various cooling time scales, so in general, protons and electrons would relax into two separate temperature distributions. In 1976, Shapiro Lightman & Eardley³⁰ (hereafter, SLE76) argued that the instability persisting at the inner region of the disk could swell this optically thick radiation pressure dominated region into an optically thin gas pressure dominated region and in this region, electrons and protons will maintain separate temperature distributions. Since flow near the BH is a two-temperature fluid, as a result research on two-temperature accretion flow started to gain prominence^{30, 31}.

Two-temperature accretion solutions as presented by SLE76 incorporated inverse-Compton processes and could produce hard radiation. However, the hydrodynamics was significantly simplified, and the accretion solutions considered were not transonic. LT80 discussed primarily about single temperature transonic flow but also briefly discussed about two-temperature solutions by assuming the ratio of ion and electron temperature to be constant. Since then, many studies were undertaken using two-temperature model. Colpi, Maraschi & Treves (1984)³² solved the two-temperature solution but by assuming freely falling matter. No transonic solutions were reported here. Similar work was done by Chakrabarti & Titarchuk (1995)³³ where only inverse-Comptonization of soft photons from the SSD, by the inner post-shock region was considered. Mandal & Chakrabarti (2005)³⁴ later extended this model for other cooling processes. In both these papers, the authors imposed a density enhancement in the flow to mimic the accretion shock. In these works, the assumption of free-fall implied that the radiative transfer was not self consistently coupled with the hydrodynamics of the system. Laurent & Titarchuk (1999)³⁵ computed the spectra from the model of Chakrabarti & Titarchuk (1995)³³, by conducting a detailed Monte-Carlo simulation of the interaction of electron gas with the soft photons from the underlying KD. In 1995, Narayan & Yi (1995),³⁶ studied self-similar class of advective solutions (termed as advection dominated accretion flow or ADAF) in the two-temperature regime. It was assumed that the amount

of heat transferred from protons to electrons through Coulomb collisions is totally radiated away. This extra assumption helped them to deal away with any kind of parametrisation, that was otherwise assumed by LT80. Needless to say self-similar class of solutions in conjunction with other assumptions mentioned above, are not transonic. Nakamura et al. (1996, 1997)^{37,38}, was among the first, who actually solved transonic two-temperature solution. However, the solutions were only for a limited class, obtained by imposing at the outer boundary, the ion temperature to be a fraction of the virial temperature and that the heat transferred to the electrons is radiated away. Manmoto et. al. (1997)³⁹ followed similar outer boundary conditions, however, in the inner region they considered that the electron energy advection rate to be equivalent to the radiative cooling rate. Rajesh & Mukhopadhyay (2010)⁴⁰ also obtained transonic solutions in the two-temperature regime, by choosing the viscosity prescription of Chakrabarti & Molteni (1995)²⁵, but only presented transonic solutions through a single sonic point. Dihingia et al. (2017)⁴¹ discussed the transonic global two-temperature solutions for smooth as well as shocked accretion solutions. All these works were in the pseudo-Newtonian regime (strong gravity is mimicked by modifying the Newtonian gravitational potential), and used two fixed adiabatic indices (Γ_e & Γ_p for electrons and protons, respectively) equation of state (EoS) of the gas. None of these works used the constants of motion (e. g., generalized Bernoulli constant) of the flow and the information of entropy close to the horizon to obtain the solutions. As discussed above, the hydrodynamics of single temperature regime is more complete and systematic. In two temperature regime, this approach is sadly lacking in the literature.

The problem with two-temperature solutions is that, without any increase in the number of governing equations, the number of flow variable increases, i.e. to say, now instead of a single temperature, one has to consider different temperatures for ion and electron. In addition, there is no known principle dictated by plasma physics which may constrain the relation between these two-temperatures in any of the boundaries. Some authors (cited above) assumed specific relations between electron heating and cooling, in order to obtain the solution. But those choices were arbitrary and cannot be considered a unique solution. Such arbitrary choices do not ‘haunt’ single temperature solution, since a transonic single-temperature solution is unique for a given set of constants of motion. Still some other authors followed the methodology of specifying the electron or ion temperature in a chosen boundary and then iterate the other flow variables to obtain a transonic solution. However, a different combination of electron and ion temperature in that boundary can give rise to another transonic solution but for the same value of generalized Bernoulli parameter^a. This would give rise to degeneracy of solutions, i. e., multiple transonic solutions for the same set of constants of motion. But nature would prefer only one and the question is which one. Moreover, the electron and the ion temperature

^ageneralized Bernoulli parameter in steady state, is a constant of motion in presence of dissipation too^{19, 21, 22}

may vary by orders of magnitude from a large distance to the horizon, so a non-relativistic EoS (i. e., EoS with fixed adiabatic indices) is untenable. However, it may also be remembered that use of relativistic EoS even in single temperature domain has been traditionally few and far between^{10,11,42}.

In this paper, we address the basic problem of finding a unique two-temperature transonic solution around BHs, in the general relativistic regime, using the two-temperature version of the Chattopadhyay-Ryu (CR) EoS^{43,44}, and how to overcome the problem, by laying down a prescription to obtain the correct solution. As far as we know, such an attempt has not been undertaken before. Using the CR EoS removes the constraint of specifying the adiabatic indices for the electron and the ion gas. In this paper, we would confine our discussion for a fully ionized electron-proton gas.

The paper is organized in the following way. In Section 2, we present the assumptions and equations used in the paper which would cover the equation of state used and the equations of motion. In Section 3, we will discuss the procedure to obtain unique transonic two-temperature solutions. In Section 4, we will present and discuss our results and finally conclude in Section 5.

2. ASSUMPTIONS AND EQUATIONS

In this paper, we focus on obtaining the unique two-temperature solution in steady state from all the degenerate solutions, which is actually difficult since plasma physics do not impose any constraint on the relation between electron and proton temperatures at any distance from the BH horizon. Therefore, we remove all frills that might complicate and obscure the question at hand. As a first simplification, we consider Schwarzschild metric i.e., the simplest BH. In order to further simplify the flow, we consider radial accretion i. e., rotation is neglected. Therefore the flow is spherical/conical. Although spherical accretion might look very simple, however, it is not entirely implausible as an accretion model. In the viscous, single temperature, rotating accretion flow regime, we have previously shown that the flow geometry in the inner region of the disc is close to conical flow with low angular momentum^{21,22}. Therefore, radial accretion might be used to mimic the inner region of AGNs and microquasars. This is to be expected too, since the BH gravity would start to dominate over other interactions in the inner accretion region around the BH, as a result a large number of papers do consider spherical flow to mimic the inner region of accretion flow^{45–47}. In addition, standard accretion model onto isolated BH from inter-stellar medium is indeed spherical^{48,49}. We consider all possible cooling mechanisms like bremsstrahlung, synchrotron and inverse-Compton processes, and it may be noted that the electron is the main agent of emission. Energy is exchanged between electrons and protons through the Coulomb interaction term given by Stepney (1983)⁵⁰. The effect of explicit heating is also discussed at the end.

It is to be noted that in the subsequent sections, all barred variables represent

6 *Shilpa Sarkar & Indranil Chattopadhyay*

dimensional quantities and all non-barred variables denote dimensionless quantities, until stated otherwise. Throughout this paper we have solved all the equations in the dimensionless domain. We have employed a unit system where, $G = M_{\text{BH}} = c = 1$, such that the unit of length is $r_g = GM_{\text{BH}}/c^2$ and time is in units of $t_g = GM_{\text{BH}}/c^3$. Here, G = Gravitational constant, M_{BH} = mass of the BH and c = speed of light.

2.1. Equations of motion

The background metric is that around a Schwarzschild BH. The non-zero components of the Schwarzschild metric are,

$$g_{tt} = -\left(1 - \frac{2}{r}\right); \quad g_{rr} = \left(1 - \frac{2}{r}\right)^{-1}; \quad g_{\theta\theta} = r^2; \quad g_{\phi\phi} = r^2 \sin^2 \theta, \quad (1)$$

The energy-momentum tensor of accretion flow is $T^{\mu\nu} = (e + p)u^\mu u^\nu + pg^{\mu\nu}$, where e is the internal energy density of the fluid and p is the isotropic gas pressure, all measured in local fluid frame, μ and ν represent the space-time coordinates and u^μ s are components of four velocities. The space component of the relativistic momentum balance equation is given by,

$$[(e + p)u^\nu u^i_{;\nu} + (g^{i\nu} + u^i u^\nu)p_{,\nu}] = 0, \quad (2)$$

The radial component of the above equation is given by,

$$u^r \frac{du^r}{dr} + \frac{1}{r^2} = -(g^{rr} + u^r u^r) \frac{1}{e + p} \frac{dp}{dr}, \quad (3)$$

The equation of conservation of particle density flux is:

$$(nu^\nu)_{;\nu} = 0, \Rightarrow \frac{1}{\sqrt{-g}} \frac{\partial(\sqrt{-g}nu^\nu)}{\partial x^\nu} = 0. \quad (4)$$

where, n is the number density of the particles in the flow and g is the determinant of the metric tensor. Integrating equation(4), we get the accretion rate which is a constant of motion throughout the flow, given by,

$$\dot{M} = 4\pi\rho u^r r^2 \cos(\theta), \quad (5)$$

where, θ is the co-latitude of the surface of the conical flow and is assumed to be $\theta = 60^\circ$ in this paper. The mass density is represented as ρ . The first law of thermodynamics is given by,

$$u^\mu \left[\left(\frac{e + p}{\rho} \right) \rho_{,\mu} - e_{,\mu} \right] = \Delta Q, \quad (6)$$

where, $\Delta Q = Q^+ - Q^-$, Q^+ being the heating term and Q^- the cooling term. The dimensional form of any quantity are written with a bar over it, \bar{Q} s are in units of $\text{ergs cm}^{-3} \text{ s}^{-1}$, until mentioned otherwise. The calculation of \bar{Q} s require the value of number density (in units of cm^{-3}). The number density is calculated

from the dimensional form of the accretion rate equation (in the dimensional form, the accretion rate is expressed in terms of Eddington rate).

Since the flow contains electrons and protons equilibrating at two different temperatures we need to use the first law of thermodynamics separately for protons and electrons unlike in the case of one-temperature flows where the Coulomb coupling being extremely strong, allows protons and electrons to settle down to a single temperature^{19–23}. These two energy equations are coupled by the Coulomb coupling term which allows protons and electrons to exchange energy. Therefore, ΔQ in the proton energy equation can be written as, $\Delta Q_p = Q_p^+ - Q_p^-$ and in the electron energy equation as, $\Delta Q_e = Q_e^+ - Q_e^-$.

If we integrate the radial component of the relativistic Euler equation (3) with the help of equation (5) and (6), we obtain the generalized Bernoulli parameter which is a constant of motion and is given by,

$$E = -hu_t \exp(X_f), \quad (7)$$

where, $X_f = \int \frac{\Delta Q_p + \Delta Q_e}{\rho h u^r} dr$. This is conserved throughout the flow even in the presence of dissipation. In case of non-dissipative flows, $X_f = 0$ and

$$E \rightarrow \mathcal{E} = -hu_t = h\gamma\sqrt{g_{tt}} \quad (8)$$

where \mathcal{E} is the canonical form of relativistic Bernoulli parameter¹⁸ for non-dissipative relativistic flow. The exact form of specific enthalpy h will be presented in the next section and γ is the Lorentz factor.

2.2. EoS and the final form of equations of motion

To solve the equations of motion mentioned in the previous section, we need an EoS which relates temperature, pressure and internal energy of the system. As discussed before we would use CR EoS⁴⁴. Since the adiabatic index is actually a function of temperature and composition, so it does not appear explicitly in the EoS. The CR EoS is inspired by the exact calculations done earlier^{51–53}. The advantage of using CR over the exact EoS is that, the form of CR is much simpler and has been shown to be equivalent⁵⁴. The explicit form of CR EoS for multi-species flow is given by,

$$\bar{e} = \sum_i \bar{e}_i = \sum_i \left[\bar{n}_i m_i c^2 + \bar{p}_i \left(\frac{9\bar{p}_i + 3\bar{n}_i m_i c^2}{3\bar{p}_i + 2\bar{n}_i m_i c^2} \right) \right], \quad (9)$$

where, i = proton (p), electron (e^-), positron (e^+) and m_i is the mass of the corresponding i^{th} species. In this paper, we consider the accretion flow to be electron-proton plasma ($e^- - p^+$). So, in the sections to follow, i would represent only protons and electrons.

We can define dimensional number density (\bar{n}), corresponding mass density ($\bar{\rho}$) and pressure (\bar{p}) present in equation (9) in the following way :

$$\bar{n} = \sum_i \bar{n}_i = \bar{n}_p + \bar{n}_e = 2\bar{n}_e, \quad (10)$$

8 *Shilpa Sarkar & Indranil Chattopadhyay*

where, \bar{n}_p =proton number density, and \bar{n}_e =electron number density (in units of cm^{-3}).

$$\bar{\rho} = \sum_i \bar{n}_i m_i = \bar{n}_e m_e + \bar{n}_p m_p = \bar{n}_e m_e \left(1 + \frac{1}{\eta}\right) = \bar{n}_e m_e \tilde{K}, \quad (11)$$

$$\bar{p} = \sum_i \bar{p}_i = \sum_i \bar{n}_i k T_i = \bar{n}_e k (T_e + T_p) = \bar{n}_e m_e c^2 \left(\Theta_e + \frac{\Theta_p}{\eta}\right), \quad (12)$$

where, $\eta = m_e/m_p$, $\tilde{K} = 1 + 1/\eta$, T_i is the temperature of the i^{th} species (in units of Kelvin) and k = Boltzmann constant. $\Theta_i = \frac{kT_i}{m_i c^2}$ is the non-dimensional temperature which has been defined w.r.t the rest-mass energy of the corresponding i^{th} species.

Using equations (10) to (12) we can simplify the EoS (9) to obtain,

$$\bar{e} = \bar{n}_e m_e c^2 \left(f_e + \frac{f_p}{\eta}\right) = \frac{\bar{\rho} c^2 f}{\tilde{K}}, \quad (13)$$

where, f_i is defined as, $f_i = 1 + \Theta_i \left(\frac{9\Theta_i+3}{3\Theta_i+2}\right)$ and $f = f_e + f_p/\eta$.

Enthalpy can be defined as,

$$\bar{h} = \frac{\bar{e} + \bar{p}}{\bar{\rho}}. \quad (14)$$

Using equation (11), (12) and (13) we can reduce the above equation into a dimensionless form as,

$$h = \frac{f + (\Theta_e + \Theta_p/\eta)}{\tilde{K}}. \quad (15)$$

The expression for polytropic index and adiabatic index for electrons and protons are given respectively as,

$$N_p = \frac{df_p}{d\Theta_p}; \quad N_e = \frac{df_e}{d\Theta_e}; \quad \Gamma_p = 1 + \frac{1}{N_p}; \quad \text{and} \quad \Gamma_e = 1 + \frac{1}{N_e}. \quad (16)$$

The definition of the radial three-velocity is $v = [-(u_r u^r)/(u_t u^t)]^{1/2}$. Simplifying equations (3–6, 9–16) we get the gradient of velocity,

$$\frac{dv}{dr} = \frac{\mathcal{N}}{\mathcal{D}}, \quad (17)$$

where,

$$\mathcal{N} = -\frac{1}{r(r-2)} + a^2 \mathfrak{P} + (\Gamma_e - 1)\mathbb{E} + (\Gamma_p - 1)\mathbb{P} \quad \text{and} \quad \mathcal{D} = \frac{v}{1-v^2} \left(1 - \frac{a^2}{v^2}\right).$$

Here, we have defined the sound speed as, $a^2 = \mathcal{G}/h\tilde{K}$.

The expressions used in \mathcal{N} and \mathcal{D} are as follows,

$$\mathcal{G} = \Gamma_e \Theta_e + \frac{\Gamma_p \Theta_p}{\eta}; \quad \mathfrak{P} = \frac{2r-3}{r(r-2)}; \quad \mathbb{E} = \frac{\Delta Q_e}{\rho h u^r}; \quad \mathbb{P} = \frac{\Delta Q_p}{\rho h u^r}$$

Substituting equations (5) , (10) to (13) in equation (6), we get the differential equation for both the proton and electron temperatures which is given by,

$$\frac{d\Theta_p}{dr} = -\frac{\Theta_p}{N_p} \left(\mathfrak{P} + \frac{1}{v(1-v^2)} \frac{dv}{dr} \right) - \frac{\mathbb{P}\eta\tilde{K}h}{N_p}, \quad (18)$$

$$\frac{d\Theta_e}{dr} = -\frac{\Theta_e}{N_e} \left(\mathfrak{P} + \frac{1}{v(1-v^2)} \frac{dv}{dr} \right) - \frac{\mathbb{E}\tilde{K}h}{N_e}, \quad (19)$$

respectively.

2.2.1. Radiative processes considered

Cooling of protons can be caused due to Coulomb interactions (\bar{Q}_{ep}) with electrons if $T_p > T_e$, or due to inverse bremsstrahlung (\bar{Q}_{ib}). The expression for Coulomb interaction term in cgs unit is given by⁵⁵ ,

$$\begin{aligned} \bar{Q}_{ep} = & \frac{3}{2} \frac{m_e}{m_p} \bar{n}_e \bar{n}_p \sigma_T c k \frac{T_p - T_e}{K_2(1/\Theta_e) K_2(1/\Theta_p)} \ln \Lambda_c \\ & \times \left[\frac{2(\Theta_e + \Theta_p)^2 + 1}{\Theta_e + \Theta_p} K_1 \left(\frac{\Theta_e + \Theta_p}{\Theta_e \Theta_p} \right) + 2K_0 \left(\frac{\Theta_e + \Theta_p}{\Theta_e \Theta_p} \right) \right], \end{aligned} \quad (20)$$

where, σ_T is the Thomson scattering cross-section, $K_i(x)$'s are the modified Bessel functions of i^{th} order and second kind, $\ln \Lambda_c$ is the Coulomb logarithm which we took to be equal to 20.

The expression for inverse bremsstrahlung is given by^{56,57} ,

$$\bar{Q}_{ib} = 1.4 \times 10^{-27} \bar{n}_e^2 \sqrt{\frac{m_e}{m_p}} T_p. \quad (21)$$

The cooling of electrons includes contributions from three radiative cooling mechanisms namely bremsstrahlung (\bar{Q}_{br}), synchrotron (\bar{Q}_{syn}) and inverse Compton scattering (\bar{Q}_{ic}). Therefore, $\bar{Q}_e^- = \bar{Q}_{br} + \bar{Q}_{syn} + \bar{Q}_{ic}$.

The expression for bremsstrahlung emissivity (in c.g.s units) is given by,⁵⁸

$$\bar{Q}_{br} = 1.4 \times 10^{-27} \bar{n}_e^2 \sqrt{T_e} (1 + 4.4 \times 10^{-10} T_e). \quad (22)$$

The cooling per unit volume in case of synchrotron radiation is given as³⁶ ,

$$\bar{Q}_{syn} = \frac{2\pi k T_e}{3c^2} \frac{\nu_c^3}{r r_g}, \quad (23)$$

where, ν_c is the critical frequency below which the emission is self-absorbed. It can be defined as $\nu_c = \frac{3}{2} \nu_o \Theta_e^2 x_M$ where $\nu_o = 2.8 \times 10^6 B$. One has to solve a transcendental equation to obtain the value of x_M . Here, B is defined as the stochastic magnetic field present in the flow, whose value is obtained by assuming its pressure ($B^2/8\pi$) to be in partial or full equipartition with the gas pressure (\bar{p}). This ratio can be defined as β and is chosen as $\beta = 0.01$, unless otherwise mentioned.

The Comptonization of the soft photons generated through synchrotron process, is given as⁵⁹,

$$\bar{Q}_{\text{ic}} = \zeta \bar{Q}_{\text{syn}}, \quad (24)$$

where, ζ is the enhancement factor which is defined as the average change in energy of the photon at escape after all scatterings. It is expressed as $\zeta = P(A - 1)(1 - PA)^{-1} \left[1 - (x_c/(3\Theta_e))^{-(1+\ln P/\ln A)} \right]$. Here, $x_c = h\nu_c/m_e c^2$, $P = 1 - \exp(-\tau_{\text{es}})$ is the probability of a photon to be scattered in a medium with optical depth τ_{es} , and $A = 1 + 4\Theta_e + 16\Theta_e^2$, is the mean amplification factor in energy of the scattered photon. The optical depth of a medium where electron-scattering is dominant is given by⁶⁰, $\tau_{\text{es}} = 0.4 \left[1 + (2.22T_e \times 10^{-9})^{0.86} \right]^{-1}$.

The plasma is heated via magnetic dissipation and it primarily affects the proton distribution, and part of this heat is transmitted to the electrons through the Coulomb coupling term. The dissipative heating rate is given by^{47,49},

$$\bar{Q}_{\text{p}}^+ \approx \bar{Q}_{\text{B}} = \frac{3cu^r}{2rr_g} \frac{B^2}{8\pi} = \frac{3cu^r}{2rr_g} \beta \bar{n}_e k(T_e + T_p). \quad (25)$$

2.2.2. Entropy accretion rate expression

From single temperature solutions we know we can define an entropy-accretion rate by integrating equations (18 & 19) by turning off the explicit heating and cooling terms.

$$\begin{aligned} \frac{d\Theta_p}{dr} &= \frac{\Theta_p}{N_p} \frac{1}{n_p} \frac{dn_p}{dr} + \frac{Q_{\text{ep}} \eta \tilde{K}}{\rho u^r N_p} \\ \frac{d\Theta_e}{dr} &= \frac{\Theta_e}{N_e} \frac{1}{n_e} \frac{dn_e}{dr} - \frac{Q_{\text{ep}} \tilde{K}}{\rho u^r N_e}. \end{aligned} \quad (26)$$

In single temperature regime, it is very easy to integrate the above equation, but now, due to the presence of Coulomb interaction term, equation (26) is not generally integrable. And therefore, we cannot have an analytical expression for the measure of entropy at every r in two-temperature solutions.

However, in regions where Q_{ep} can be neglected, an analytical expression is admissible. Such a region is just outside the horizon, where gravity overwhelms any other interaction. So, near the horizon, where Q_{ep} is negligible, equations (26) can be integrated to obtain,

$$n_{\text{ein}} = \kappa_1 \exp\left(\frac{f_{\text{ein}} - 1}{\Theta_{\text{ein}}}\right) \Theta_{\text{ein}}^{\frac{3}{2}} (3\Theta_{\text{ein}} + 2)^{\frac{3}{2}} \quad (27)$$

$$n_{\text{pin}} = \kappa_2 \exp\left(\frac{f_{\text{pin}} - 1}{\Theta_{\text{pin}}}\right) \Theta_{\text{pin}}^{\frac{3}{2}} (3\Theta_{\text{pin}} + 2)^{\frac{3}{2}}, \quad (28)$$

where, κ_1 and κ_2 are the integration constants which are a measure of entropy. We know from charge neutrality condition that $n_{\text{ein}} = n_{\text{pin}} = n_{\text{in}}$. Subscript ‘in’

indicates quantities measured just outside the horizon. Therefore we can write,

$$\begin{aligned}
 n_{\text{in}}^2 &= n_{\text{ein}} n_{\text{pin}} \\
 \Rightarrow n_{\text{in}} &= \sqrt{n_{\text{ein}} n_{\text{pin}}} \\
 &= \kappa \sqrt{\exp\left(\frac{f_{\text{ein}} - 1}{\Theta_{\text{ein}}}\right) \exp\left(\frac{f_{\text{pin}} - 1}{\Theta_{\text{pin}}}\right) \Theta_{\text{ein}}^{\frac{3}{2}} \Theta_{\text{pin}}^{\frac{3}{2}}} \\
 &\quad \times \sqrt{(3\Theta_{\text{ein}} + 2)^{\frac{3}{2}} (3\Theta_{\text{pin}} + 2)^{\frac{3}{2}}}, \tag{29}
 \end{aligned}$$

where, $\kappa = \sqrt{\kappa_1 \kappa_2}$

Thus, the expression of entropy accretion rate can be written as,

$$\begin{aligned}
 \dot{\mathcal{M}}_{\text{in}} &= \frac{\dot{M}}{4\pi\kappa(m_e + m_p)\cos(\theta)} \\
 &= \sqrt{\exp\left(\frac{f_{\text{ein}} - 1}{\Theta_{\text{ein}}}\right) \exp\left(\frac{f_{\text{pin}} - 1}{\Theta_{\text{pin}}}\right) \Theta_{\text{ein}}^{\frac{3}{2}} \Theta_{\text{pin}}^{\frac{3}{2}}} \\
 &\quad \times \sqrt{(3\Theta_{\text{ein}} + 2)^{\frac{3}{2}} (3\Theta_{\text{pin}} + 2)^{\frac{3}{2}}} u^r r^2 \tag{30}
 \end{aligned}$$

In section 4.2, we will use equation (30) to obtain the correct accretion solution.

2.2.3. Sonic point conditions

As argued before, black hole accretion is transonic in nature. So, at some $r = r_c$ the critical point, the flow $dv/dr \rightarrow 0/0$. This condition gives us the critical point conditions. Thus using equation (17) we get,

$$-\frac{1}{r_c(r_c - 2)} + a_c^2 \mathfrak{P}_c + (\Gamma_{ec} - 1)\mathbb{E}_c + (\Gamma_{pc} - 1)\mathbb{P}_c = 0, \tag{31}$$

and,

$$\frac{v_c}{1 - v_c^2} \left(1 - \frac{a_c^2}{v_c^2}\right) = 0. \tag{32}$$

Here, ‘c’ in the subscript resembles the values of the variables at the critical point. At r_c , the radial three-velocity is equal to the sound speed or $v_c = a_c$, i. e., the Mach number $M_c = v_c/a_c = 1$. Since the derivative of velocity at the critical point has a 0/0 form, therefore it is calculated using l’Hospital rule.

3. SOLUTION PROCEDURE

It has already been established by Bondi (1952)², that for a given boundary condition the entropy of the transonic global solution is maximum, and therefore, a transonic solution is the solution favoured by nature. Therefore, we look for a transonic solution. The general procedure to find a solution in two-temperature is similar to the one in the single temperature regime, which is — for a given set of flow parameters (E, \dot{M}) , the sonic point is obtained first, and then integrate the gradient

of velocity and temperature, that is equations (17), (18) and (19), from the sonic point inwards and outwards, in order to obtain self-consistent values of v , Θ_p and Θ_e respectively throughout the flow. A spherical flow harbours only a single sonic point.

3.1. *Method to find the sonic point: single temperature versus two temperature*

This is the first step in obtaining a general transonic solution. Finding a sonic point is not trivial in presence of heating and cooling. To find the sonic points we need to first choose a boundary: horizon or infinity. The advantage of choosing the horizon as the boundary, is that atleast the inflow velocity on the horizon is known ($v_{\text{in}} = c$), while at the outer boundary its value is arbitrary. Unfortunately, there is a coordinate singularity on the horizon, so one cannot start the integration from the horizon. Therefore, we chose a location asymptotically very close to the horizon, $r_{\text{in}} \rightarrow 2r_g$. Very close to the horizon gravity overwhelms all other interactions, therefore the flow becomes adiabatic, i. e., as $r_{\text{in}} \rightarrow 2r_g$, $E \rightarrow \mathcal{E}$. At r_{in} for single temperature flow, there are two unknowns v_{in} and the temperature. So for a given E , at r_{in} we supply a temperature in the expression of $E = \mathcal{E}$ to obtain a value of velocity, say v'_{in} . With these values of velocity and temperature we integrate the equations of gradient of velocity, and temperature to obtain a solution and check for sonic point conditions. If the solution does not pass through the sonic point, then we change the temperature supplied at r_{in} and repeat the process until and unless for a certain temperature at r_{in} we obtain a $v_{\text{in}} = v'_{\text{in}}$ which on integration satisfies the sonic point conditions at some $r = r_c$. Therefore, we obtain a transonic solution by iterating the temperature to give us the unique transonic solution. This is in essence a variation of the solution procedure of Becker and his collaborators.

For two-temperature flow however, we have three unknowns, v_{in} , Θ_{ein} and Θ_{pin} at r_{in} , and still two constants of motion E and \dot{M} . That is, the number of variables increases by one, while the number of equations, or equivalently the number of constants, remains the same as we had in the single temperature regime. So for a given E and \dot{M} , we supply Θ'_{pin} , Θ'_{ein} at r_{in} and compute v'_{in} from the expression of E . Considering Θ'_{pin} , Θ'_{ein} and v'_{in} as guess values of temperatures and flow velocity near the horizon, we integrate equations (17, 18 & 19) outwards and check for sonic point conditions (equations 31, 32). If the sonic point condition is not satisfied, then we change the value of Θ'_{ein} , obtain another value of v'_{in} and again we integrate the same equations. Similarly we also change Θ'_{pin} and repeat the same procedure again, if no transonic solution is obtained. If the sonic point is found out, then the transonic solution with those values of $\Theta_{\text{pin}} = \Theta'_{\text{pin}}$, $\Theta_{\text{ein}} = \Theta'_{\text{ein}}$ and $v_{\text{in}} = v'_{\text{in}}$ for that particular set of E and \dot{M} , is the solution. We have chosen $r_{\text{in}} = 2.001r_g$. One has to remember however, now the system is under determined, the consequence of which will be seen in the next section. It may be further noted that, we mentioned Θ_{pin} is supplied to iterate Θ_{ein} and v_{in} from E , however while presenting results,

we prefer to quote T_{pin} or T_{ein} instead. This will make it easier for the reader to relate to the problem.

4. RESULT

We initially assume $Q_p^+ = 0$ to discuss various features of two-temperature solution. The effect of $Q_p^+ \neq 0$ will be discussed later in section 4.5.

4.1. Investigating degeneracy in two-temperature flows

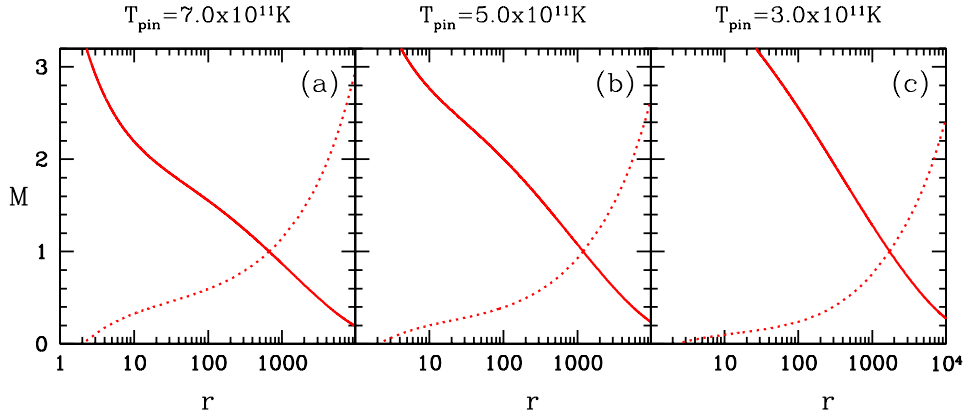


Fig. 1. (a) Accretion M (solid, red) and wind M (dotted, red) as a function of r corresponding to $M_{\text{BH}} = 10M_{\odot}$, $\dot{M} = 0.01$ and $E = 1.0001$. The different solutions are obtained changing T_{pin} (values are written on the top of each panel).

In Figs.(1a, b, c), we present the accretion solutions of two-temperature Bondi flow for $M_{\text{BH}} = 10M_{\odot}$, $\dot{M} = 0.01$ and $E = 1.0001$. Each panel shows the accretion Mach number or $M = v/a$ (solid, red) and corresponding wind M (dotted, red) as a function of r . The crossing points are the location of sonic/critical points. The three solutions plotted in the figure are obtained by changing the proton temperature T_{pin} ($T_{\text{pin}} = T_p|_{r \rightarrow r_{\text{in}}}$), but for the same E and \dot{M} for a given central BH. This implies that different values of T_{pin} would yield different solutions, each with a unique sonic point position and sonic point properties. In section 3.1, we pointed out that the two-temperature regime is under determined, because we need to know three unknowns at r_{in} but there were only two constants of motion. The degeneracy in solution is the direct fall out of such a scenario. All transonic two-temperature solutions, whether in exact GR or in pseudo-Newtonian regime, suffers from this deficiency. In the next section we will discuss, the physical principle to be followed in order to obtain a unique two-temperature transonic solution.

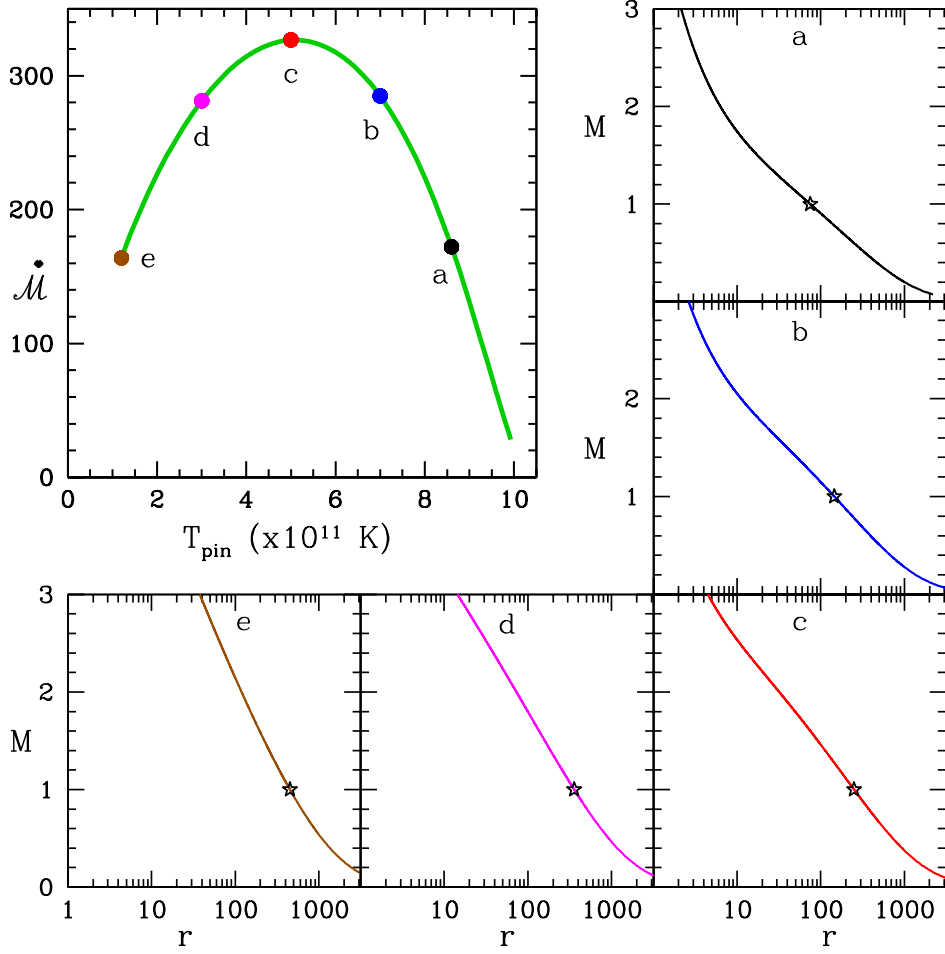


Fig. 2. Top left panel: Variation of \mathcal{M}_{in} as a function of T_{pin} for accretion flow of $\dot{M} = 0.1$ and $E = 1.001$ onto a $10M_{\odot}$ BH. Panels 'a' to 'e' presents M of the accretion (solid) with r corresponding to each of the points 'a'—'e' on the $\mathcal{M}_{\text{in}}-T_{\text{pin}}$ curve. The stars show the location of sonic points. At $T_{\text{pin}} = 5.0 \times 10^{11}$ K (marked 'c') entropy maximizes, so panel 'c' is the correct solution for the given E and \dot{M} .

4.2. Entropy measure as a tool to remove degeneracy in two-temperature flows

As has been shown in Fig. (1a—c), for a given set of constants of motion namely E and \dot{M} , there can be a plethora of transonic solutions, each differentiated by the T_{pin} at r_{in} . Now the only way this degeneracy can be removed is by invoking the second law of thermodynamics. It has also been shown in section 2.2.2, that a general analytical expression of entropy measure is not possible, however, the entropy of the accreting matter very close to the BH can be calculated (equation 30). So in Fig. (2, top left panel) we plot the measure of entropy \mathcal{M}_{in} at $r = r_{\text{in}}$ as a

function of T_{pin} , for an accretion flow characterized by constants of motion $\dot{M} = 0.1$ and $E = 1.001$ on to a BH of $M_{\text{BH}} = 10M_{\odot}$. We have marked points ‘a’ to ‘e’ on the $\dot{\mathcal{M}}_{\text{in}}$ vs T_{pin} curve, and then have plotted the corresponding solutions (M vs r) in the adjacent panels also named as ‘a’ to ‘e’. It is easy to notice that the solutions are completely different since, the sonic points of the solutions vary by a few $\times 100r_{\text{g}}$ for this particular E and \dot{M} . In particular, solution marked ‘a’ and that marked ‘e’ both have the same $\dot{\mathcal{M}}_{\text{in}}$ and E , but the sonic point of ‘a’ is at $r_c = 75.008$ and that of ‘e’ is at $r_c = 451.297$, respectively. Different proportions of T_e and T_p might give rise to the same $\dot{\mathcal{M}}_{\text{in}}$ and E ! This also implies a wrong choice of solution would lead us to wrong conclusions about the physical processes around BHs. *However, only one of them is correct.* It must be noticed that, of all the solutions, the entropy distribution has single well behaved maxima at $T_{\text{pin}} = 5 \times 10^{11}\text{K}$, and therefore, by the second law of thermodynamics, the accretion solution corresponding to this entropy at point ‘c’ on the curve is the correct one.

4.3. Properties of unique two-temperature transonic solution

4.3.1. Critical point properties:

For adiabatic flow, sonic points can be found directly from a given value of E , but in our case the sonic point can be obtained only after obtaining the solution. Since the system is under determined, unique r_c can only be obtained by invoking the second law of thermodynamics. Taking all these factors into consideration, we plot E as a function of r_c (Figs. 3a); while v_c (Fig. 3b); Γ_{pc} , Γ_{ec} (Fig. 3c) and $\dot{\mathcal{M}}_{\text{in}}$ (Fig. 3d) as functions of E . Each curves are for accretion rate $\dot{M} = 0.01$ (yellow-solid), 0.10 (red-dotted), 0.50 (magenta-dashed), 1.00 (green - long-dashed) and 5.00 (blue - dot-dashed). Here a BH of $10M_{\odot}$ has been considered. For low accretion rates ($\dot{M} \leq 0.1$), the range of sonic points are $3 < r_c \rightarrow \infty$, however, for higher accretion rates, the sonic point range decreases significantly. In presence of significant cooling (i. e., higher \dot{M}), hot flows from large distance can be accreted, which otherwise could not be accreted. As a result v_c and the entropy both are higher for flows with higher \dot{M} . From all the plots it is clear that, for spherical accretion, there can be only one sonic point.

4.3.2. Flow variables and emissivity

In Fig.(4a-f) we present various flow variables of the correct Bondi accretion on to a BH $M_{\text{BH}} = 10M_{\odot}$. The constants of motions are $E = 1.00001$ and $\dot{M} = 0.01$. The flow variables plotted are M , E , T_p & T_e , Γ_e & Γ_p and v on the panels Fig.(4a-e), respectively. The star mark indicates the location of sonic point. **Figure (4b) shows that** the generalized Bernoulli parameter E is indeed a constant of motion. It is also to be noted that, $T_e \approx T_p$ (solid, Fig. 4c) at large r and $T_e < T_p$ at $2 < r < 1000$. Moreover, the electron fluid while traveling a distance of about $10^4 r_{\text{g}}$ on the way to the BH, spans a temperature range of more than two or-

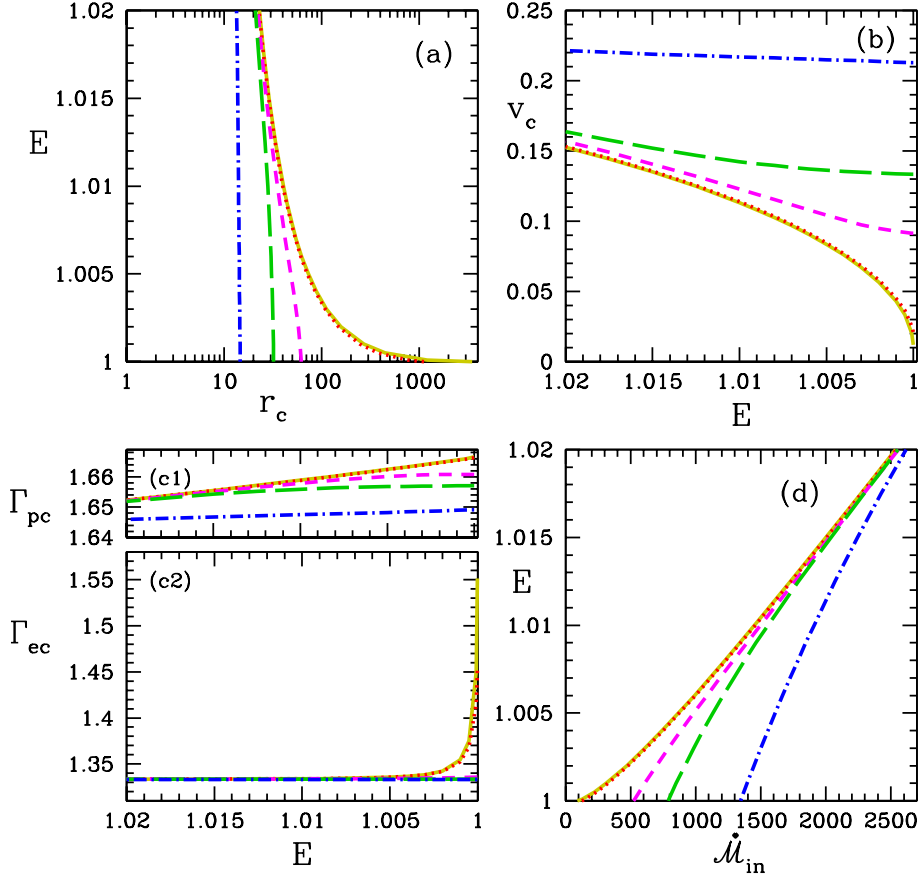


Fig. 3. Variation of sonic points and its properties with the accretion rate (\dot{M}) of the BH. Here we have assumed $M_{BH} = 10M_{\odot}$. We have taken $\dot{M} = 0.01$ (yellow-solid), 0.10 (red-dotted), 0.50 (magenta-dashed), 1.00 (green - long-dashed) and 5.00 (blue - dot-dashed).

ders of magnitude which means $1.6 > \Gamma_e \sim 4/3$ and do not have any constant value. In addition, $1.6 < \Gamma_p \sim 5/3$ and the temperature of the proton fluid spans more than three orders of magnitude. But the distribution of Γ_e & Γ_p would also change for a different set of constants of motion (E , \dot{M}). In other words, considering CR EoS is important. In Fig.(4 f), we plot the total electron emissivity or Q_e^- , bremsstrahlung (Q_{br}), synchrotron (Q_{syn}), inverse-Compton (Q_{ic}), inverse-bremsstrahlung (Q_{ib}) and Coulomb coupling term (Q_{ep}) as a function of distance. All the Q s used are in physical units ($\text{ergs cm}^{-3} \text{s}^{-1}$), and for simplicity \bar{Q} are not used. Q_{br} dominates the radiative process for this particular set of E and \dot{M} , except near the horizon where the $Q_{syn} \gtrsim Q_{br}$. Q_{ic} is quite weak for low accretion rate. Q_{ib}

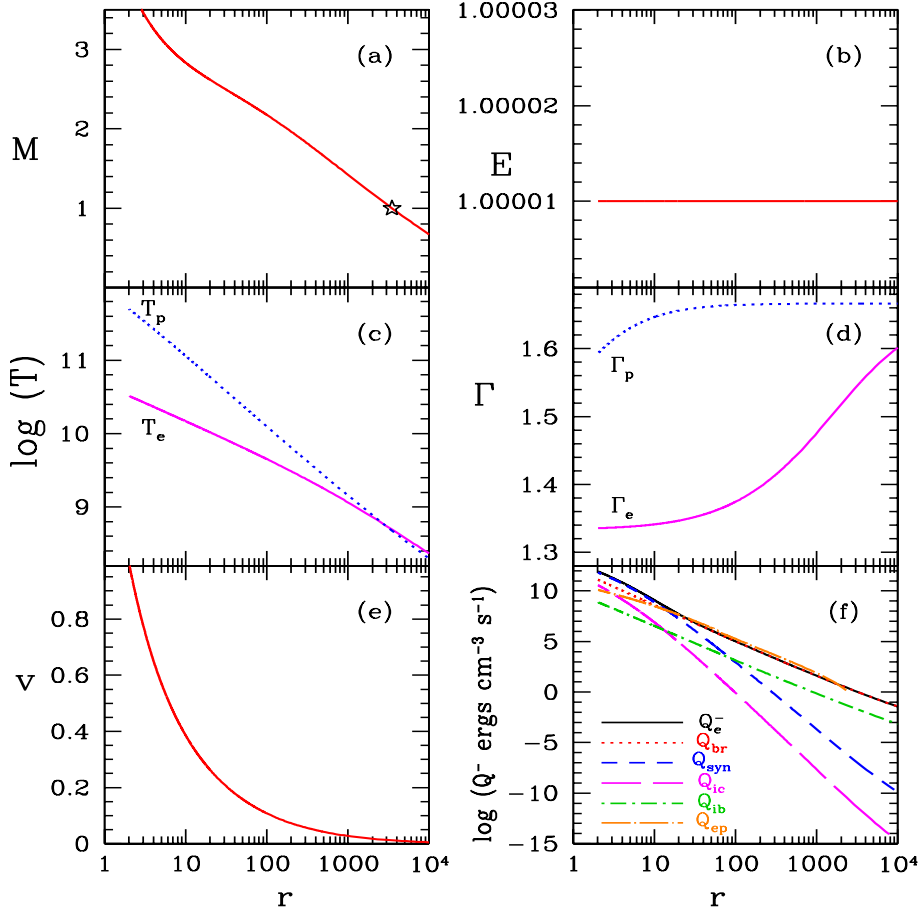


Fig. 4. Variation of (a) M ; (b) E ; (c) T_p and T_e ; (d) Γ_e and Γ_p ; (e) v ; and (f) total (Q_e^-), bremsstrahlung (Q_{br}), synchrotron (Q_{syn}), inverse-Compton (Q_{ic}), and inverse-bremsstrahlung (Q_{ib}) emissivities as a function of r . The Coulomb coupling Q_{ep} is over plotted. The star on the M distribution represent the location of the sonic point r_c . The accretion disc parameters are $E = 1.00001$, $M_{BH} = 10M_\odot$ and $\dot{M} = 0.01$. The Q s presented, are in physical units ($\text{ergs cm}^{-3} \text{s}^{-1}$).

may have larger contribution than Q_{syn} or Q_{ic} at larger distance, but $Q_{ib} \ll Q_e^-$. Since Q_{ep} is also comparable to Q_e^- except near the horizon, T_p and T_e is comparable in a large range of r . Close to the horizon, $Q_{ep} \ll Q_e^-$ as a result $T_p \gg T_e$. On careful inspection it is clear that at $r > 2000r_g$, $Q_{ep} < 0$ and therefore $T_e > T_p$. So one can say, attainment of single temperature distribution or, two-temperature distribution depends on the relative strength of Coulomb interaction and various radiative processes.

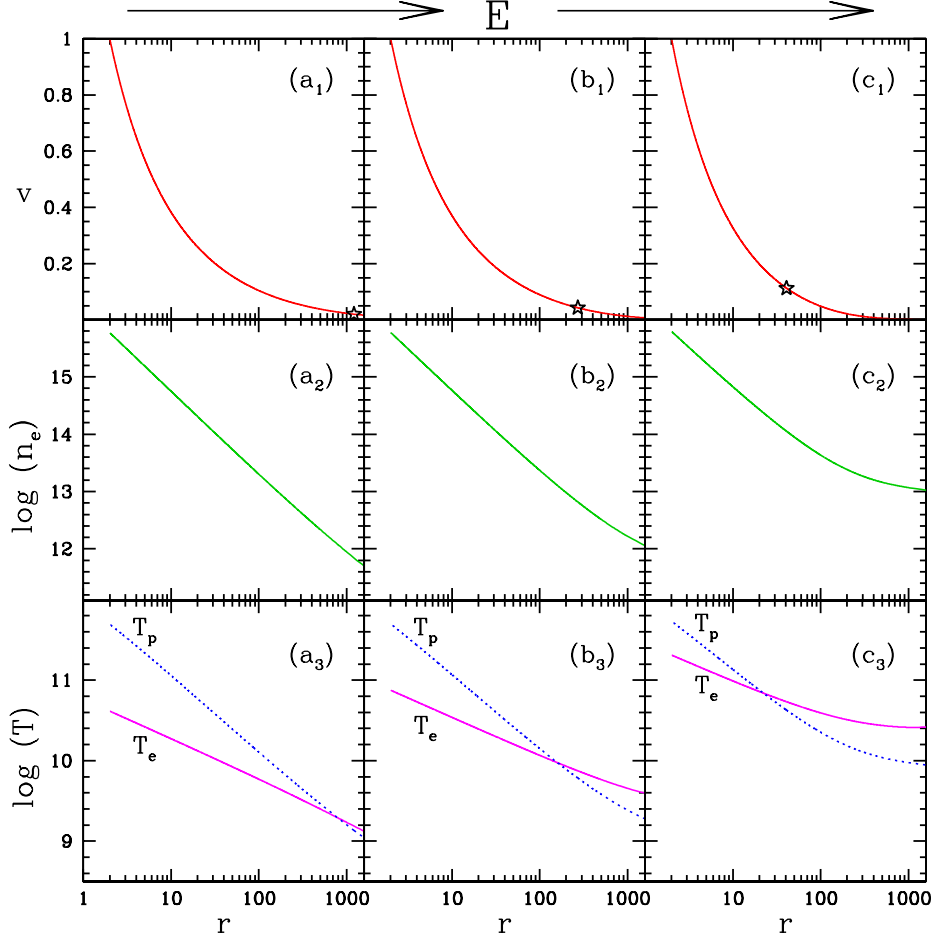


Fig. 5. Variation of v (a_1, b_1, c_1); electron number density n_e (a_2, b_2, c_2) and T_p & T_e in panels (a_3, b_3, c_3), as a function of r . The generalized Bernoulli parameter changes from the left panels $E = 1.0001$ (a_1, a_2, a_3), to the middle panels $E = 1.001$ (b_1, b_2, b_3) and then to the right panels $E = 1.01$ (c_1, c_2, c_3). Other parameters selected are $M_{\text{BH}} = 10M_{\odot}$ and $\dot{M} = 0.01$.

4.3.3. Dependence of accretion flow on E and \dot{M}

In Figs.(5a₁-c₃) we show how the global transonic two-temperature solutions depend on constant of motion E (increases left to right) for a given \dot{M} on to a stellar mass BH. We have plotted v (a_1, b_1, c_1); electron number density n_e (a_2, b_2, c_2) and T_p & T_e in panels (a_3, b_3, c_3), as a function of r . The star on the velocity curve shows the location of sonic point. For higher E , r_c is formed closer to the horizon. Increasing E , raises the temperature at the outer boundary and reduces v , thus the electron number density at the outer boundary is also higher for higher E .

Increasing \dot{M} has similar effect on the accretion solutions. We plot the velocity

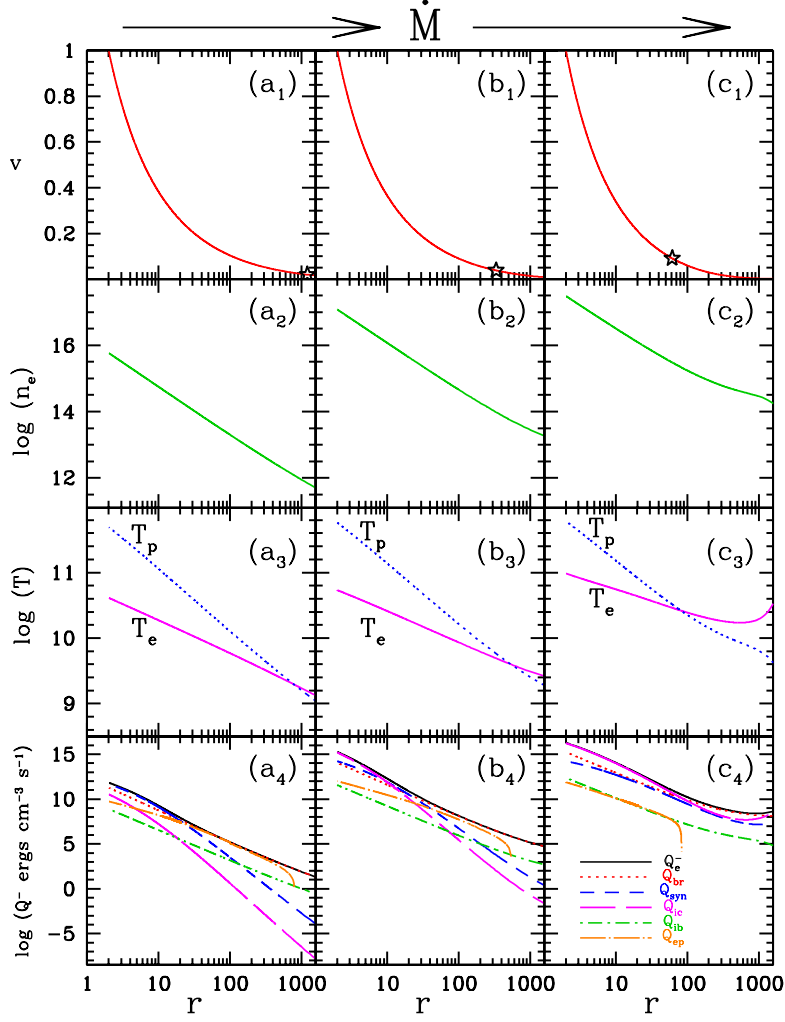


Fig. 6. Variation of v (a_1, b_1, c_1); electron number density n_e (a_2, b_2, c_2), T_p & T_e in panels (a_3, b_3, c_3) and various radiative emissivities and Q_{ep} (a_4, b_4, c_4) in panels as a function of r . The accretion rate changes from the left panels $\dot{M} = 0.01$ (a_1, a_2, a_3, a_4), to the middle panels $\dot{M} = 0.2$ (b_1, b_2, b_3, b_4) and then to the right panels $\dot{M} = 0.5$ (c_1, c_2, c_3, c_4). Other parameters selected are $M_{BH} = 10 M_\odot$ and $E = 1.0001$. All Q s are presented in physical units ($\text{ergs cm}^{-3} \text{s}^{-1}$).

distribution (Fig. 6 a_1, b_1, c_1), n_e (Fig. 6 a_2, b_2, c_2), T_e & T_p (Fig. 6 a_3, b_3, c_3) and different radiative emissivities and Q_{ep} (Fig. 6 a_4, b_4, c_4) as a function of r . Once again Q s presented in this figure are in physical units and we do not put ‘bar’ in order, not to make the figure clumsy. Keeping $E = 1.0001$ constant, we change $\dot{M} = 0.01$ ($a_1 - a_4$), to $\dot{M} = 0.2$ ($b_1 - b_4$) and then to $\dot{M} = 0.5$ ($c_1 - c_4$).

Emission increases with the increase in \dot{M} , and therefore can accrete hotter flow at large distances. As a result the sonic points form closer to the horizon, even for same E . The sonic point in the figure can also be seen to move closer to the horizon (the star mark in the velocity distribution). For low \dot{M} , Q_{br} dominates (see also Fig. 4 f). Interestingly, for a distance range of $20 < r < 1000$, $Q_{\text{ep}} \approx Q_{\text{e}}^-$ (long dashed-dot). Since Coulomb interaction is comparable to the bremsstrahlung emission, $T_{\text{e}} \approx T_{\text{p}}$ in the same range. As the accretion rate increases, inverse-Compton cooling becomes more efficient and dominates in the overall emissivity (Fig. 6b₄). The Q_{ep} term becomes less effective, as a result the difference between T_{e} and T_{p} increases. For even higher \dot{M} (Fig. 6c₄), inverse-Compton dominates the cooling and Coulomb term becomes even weaker and therefore T_{e} and T_{p} becomes significantly different from each other. In fact, Coulomb coupling is effective when emission process is not very strong.

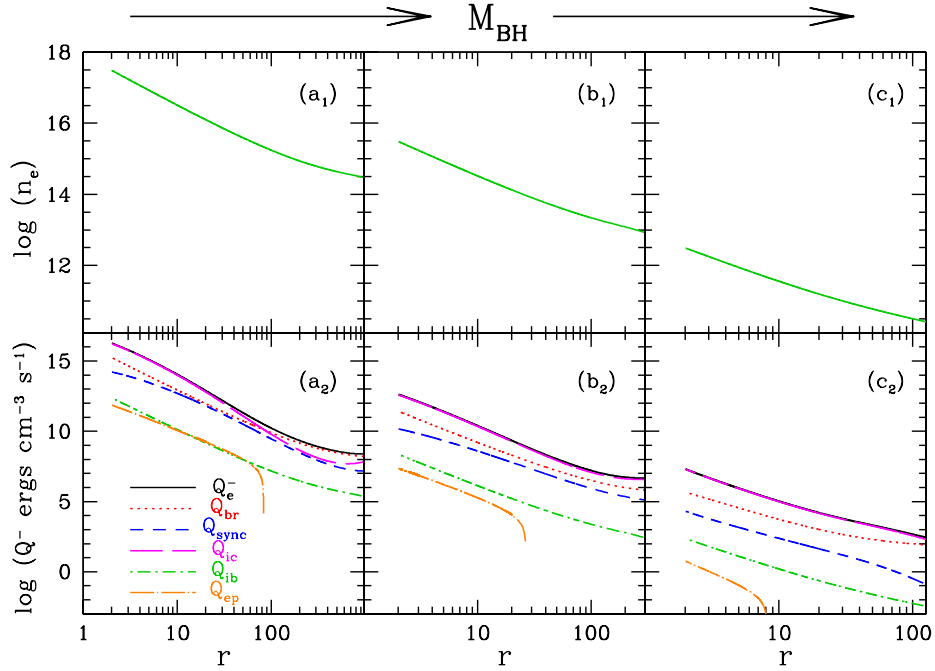


Fig. 7. Variation of n_{e} (a₁, b₁, c₁); emissivities and Coulomb coupling (a₂, b₂, c₂) as function of r . Left column panels (a₁ and a₂) are for $M_{\text{BH}} = 10 M_{\odot}$, the middle column are for $M_{\text{BH}} = 10^3 M_{\odot}$ (b₁, b₂) and for right column $M_{\text{BH}} = 10^6 M_{\odot}$ (c₁, c₂). Other parameters selected are $E = 1.0001$ and $\dot{M} = 0.5$. The Q s are in physical units ($\text{ergs cm}^{-3} \text{s}^{-1}$).

4.3.4. Effect of the mass of the central BH

Since the mass supplied is described in the units of Eddington rate, so the net amount of mass flux increases with the central mass of the BH. The number density is proportional to the inverse of M_{BH} , but the volume would increase as M_{BH}^3 . Therefore, emissivity is proportional to M_{BH}^{-2} . As a result net radiative cooling increases with M_{BH} . This allows hotter matter to flow onto a more massive BH, which pushes the sonic point closer to horizon even for matter starting with same E and \dot{M} (in units of Eddington rate). We plot n_e (Fig. 7a₁, b₁, c₁) and Q_e^- , Q_{br} , Q_{syn} , Q_{ic} , Q_{ib} , Q_{ep} (Fig. 7a₂, b₂, c₂) as a function of r , but for different $M_{\text{BH}} = 10M_{\odot}$ (Fig. 7a₁, a₂), $M_{\text{BH}} = 10^3M_{\odot}$ (Fig. 7b₁, b₂) and $M_{\text{BH}} = 10^6M_{\odot}$ (Fig. 7c₁, c₂). The Q s are presented in physical units. The sonic point for $M_{\text{BH}} = 10M_{\odot}$ is at $r_c = 61.535$, for $M_{\text{BH}} = 10^3M_{\odot}$ the $r_c = 39.966$ and finally for $M_{\text{BH}} = 10^6M_{\odot}$ the sonic point is at $r_c = 19.786$. So it is clear that radial accretion onto larger BH, is hotter and will be more luminous than the smaller ones. For low accretion rates where the number density is lower, Q_{ic} is generally lower than Q_{br} or Q_{syn} . But for higher \dot{M} accretion, Q_{ic} starts to dominate in the inner region. And since accreting larger BHs are more luminous, the total emissivity is dominated by Q_{ic} . These plots also shows that, for lower mass BH and higher \dot{M} , Q_{syn} is similar to Q_{br} , however, for higher M_{BH} , Q_{br} is much stronger than Q_{syn} . Whatever may be the mass of the central BH or accretion rate, Q_{ib} is significantly lower than the net emissivity. The Coulomb coupling term Q_{ep} is negligible for high \dot{M} and decreases even more for flow around massive BHs.

4.4. Luminosity and efficiency of the systems

Shapiro (1973)⁷ computed luminosity from Bondi flow via only the bremsstrahlung process, and concluded that radial flow is not efficient enough. However, that accretion model was not strictly two-temperature. Moreover, all classes of solutions were not investigated. From Figs. (4 — 6) of this paper, it is quite clear that the different cooling processes start to dominate at different \dot{M} . For lower \dot{M} inverse-Compton is not a very dominant process, while for higher accretion rate, inverse-Compton becomes important. Therefore, it can be safely assumed that both luminosity and efficiency of the accretion flow would also depend on the accretion rates.

In Fig. 8, panel (a), we plot the variation in luminosity (L) in units of ergs s^{-1} , with \dot{M} for accretion flow on to $M_{\text{BH}} = 10M_{\odot}$ (dotted, blue), and $M_{\text{BH}} = 10^8M_{\odot}$ (solid, red). Other parameter of the flow is $E = 1.001$. The efficiency of a BH system can be written as $\epsilon = L/(\dot{M}c^2)$. In Fig. (8 b), the corresponding ϵ is plotted as a function of \dot{M} . For low $\dot{M} \lesssim 0.2$, the efficiency of conversion of accretion energy to radiation is really low $\epsilon \lesssim 0.01$ for both kind of BHs. However, for $\dot{M} > 0.5$ the efficiency $\gtrsim 0.1$ for accretion on to 10^8M_{\odot} BH and comfortably produces $L \gtrsim 10^{44}\text{ergs s}^{-1}$. At super Eddington accretion rates super massive BH produces luminosities above $10^{45}\text{ erg s}^{-1}$ with efficiency $\epsilon \sim 0.2$. Accretion flow on to stellar mass BH can emit at $L \sim 10^{38}\text{erg s}^{-1}$ for $\dot{M} \gtrsim 0.8$. However, the

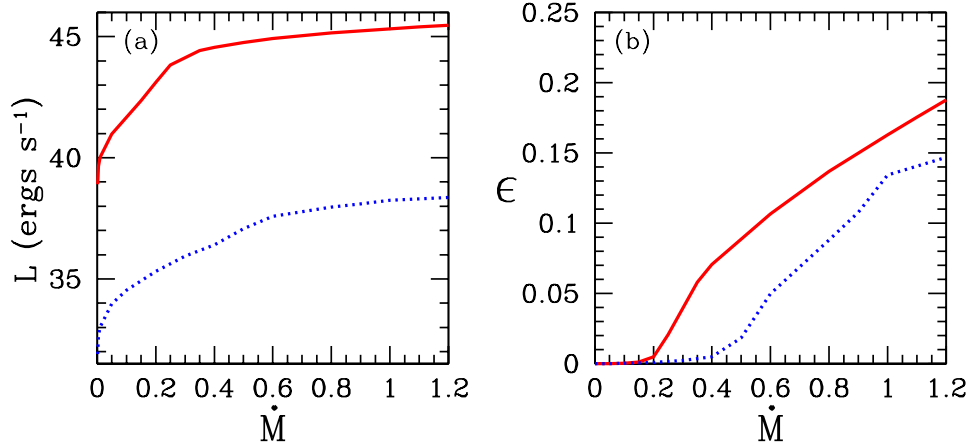


Fig. 8. (a) Luminosity L , and (b) efficiency ϵ as a function of \dot{M} . Each curve corresponds to $M_{\text{BH}} = 10^8 M_{\odot}$ (solid, red) and $M_{\text{BH}} = 10 M_{\odot}$ (dotted, blue). Other parameter is $E = 1.001$.

efficiency of accretion flow around stellar mass BH is generally lower than the one around super-massive BH, however, for $\dot{M} > 0.8$ the efficiency $\epsilon > 0.1$. So not only the accretion flow onto massive BHs are brighter, even its radiative efficiency is more.

4.5. Effect of dissipative proton heating

So far in this paper we considered no explicit heating. We now consider dissipative magnetic heating in the footsteps of Ipser & Price (1982)⁴⁷. It mainly affects the protons, however, through Coulomb coupling the dissipated energy is also transmitted to the electrons. In Fig. (9a₁—a₃), we plot v (panel a₁), temperatures (panel a₂) and various emissivities, heating rate and the Coulomb coupling term (panel a₃). Comparing with Fig. (5b₁—b₃), which was for the same accretion parameters but without heating, the effect of heating is clearly seen. The sonic point in the present case is pushed back, i.e., BH is accreting matter with lower temperatures at the outer boundary. Since the \dot{M} is low, so the heating term Q_p^+ dominates. In Fig. (9b₁—b₃) the same variables are plotted but now for higher $\dot{M} = 0.5$. In this case the Q_e^- dominates over Q_p^+ . The Coulomb coupling on either case is negligible. Heating processes quantitatively affects the solutions, if the dissipative heat only directly affects the protons. This is because, in general Coulomb coupling is not very effective in energy exchange between electrons and protons and was also suggested by Manmoto et. al (1997).³⁹

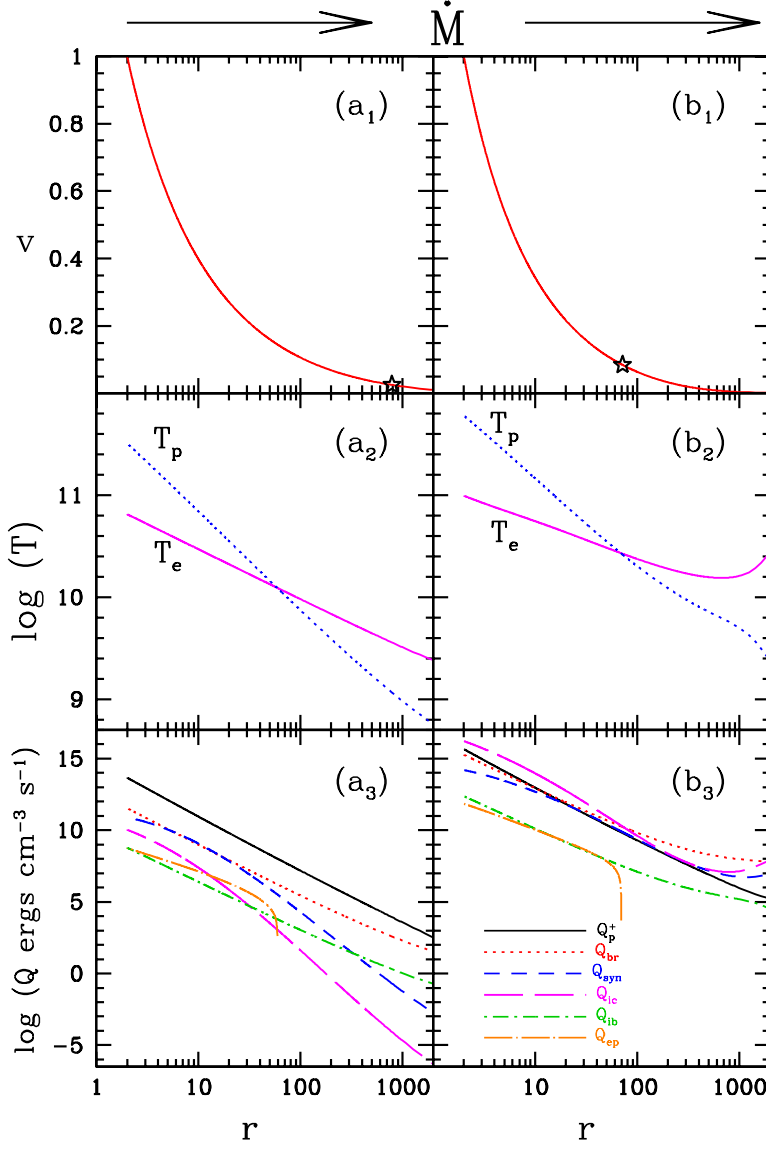


Fig. 9. Three-velocity v (a₁, b₁), temperatures (a₂, b₂) and emissivities, heating and Coulomb coupling (a₃, b₃) as a function of r . The solutions are for $\dot{M} = 0.01$ (a₁–a₃) and $\dot{M} = 0.5$ (b₁–b₃). Other parameters are for $E = 1.001$ and $M_{\text{BH}} = 10M_{\odot}$.

5. DISCUSSIONS AND CONCLUSIONS

A correct two-temperature solution is very important, because a proper electron temperature distribution for a given boundary condition, produces the correct spectrum and luminosity. Moreover, analytical solutions obtained in this paper is also

important since, these solutions may act as tests, as well as, may be used as initial conditions for simulation codes.

Although there are few papers in the single temperature regime, which used constants of motion to obtain the solutions, but as far as we know, probably there are none in the two-temperature domain which even addresses the issue of constants of motion while obtaining the solutions. It may be remembered that, a fluid solution is not just characterized by its energy but also its entropy, and according to the second law of thermodynamics, any physical solution should correspond to the one with highest entropy. It was Bondi² who used this principle in order to stress that a transonic solution is the correct accretion solution under the influence of gravity. Later Becker and his collaborators^{26–29} used the information of energy as well as the entropy to obtain transonic accretion solutions around a black hole in presence of dissipation. Since the set of equations in single temperature flow is complete, so finding a transonic solution suffices the criteria for second law of thermodynamics. However, as has been discussed extensively in the paper, the set of governing equations are less than the number of variables, second law of thermodynamics becomes essential even to find a proper solution. The novelty of this work is to identify this problem and laying down the procedure to overcome it, by actually following the footsteps of Bondi and Becker.

In this paper, we obtained the expression for the generalized Bernoulli parameter (E) for two temperature flow, by integrating the energy-momentum balance equation and showed that it is indeed a constant of motion. Moreover, integrating the continuity equation we obtained the expression for accretion rate (\dot{M}) which is the other constant of motion. In addition, we explicitly showed that degenerate transonic solutions exist for a given set of constants of motion. To remove the degeneracy we took the help of the second law of thermodynamics near the horizon, according to which the transonic solution which has maximum entropy should be the solution. The next hurdle was, that there was no analytical expression of entropy measure for two-temperature flow. We used the BH inner boundary condition (gravity overwhelms all other interactions), in order to obtain the analytical expression of entropy measure (\mathcal{M}_{in}) for a gas in two-temperature regime valid only near the horizon and that too, by using relativistic EoS.

To focus on the problem of degenerate two-temperature solutions and its possible remedy, we considered a simple accretion model of radial flow onto a black hole. More complicated accretion model would have obscured the crux of the problem. Simple as it may be, but spherical accretion is preferred mode of accretion onto isolated BHs immersed in interstellar matter and has been shown by many authors^{48,49}. Moreover, the inner region of a BH accretion disc is also quasi spherical and many researchers have considered radial inflow to mimic inner accretion disc^{45,46}. Since radial flow has no angular momentum (quasi spherical flow may have minuscule amount), viscous transport should be negligible for accretion onto isolated BH or in the inner region of an accretion disc. Moreover, authors who have obtained transonic two-temperature solution before³⁹, are of the view that Coulomb

coupling is not an efficient energy transfer process. Therefore any viscous heating will anyway not find its way into heating up the electrons. Looking into all these factors, we ignored viscous dissipation and concentrated two-temperature accretion flow by only considering cooling mechanisms in this paper. However, at the end we did consider dissipative proton heating⁴⁷. Heating has quantitative effect on the accretion solutions and confirmed that Coulomb coupling is weak as was mentioned by Manmoto et. al. (1997)³⁹.

Using the methodology explained above, we obtained all possible solutions for any given set of E and \dot{M} . For higher E and higher \dot{M} , sonic points were formed closer to the horizon, while for lower values of both the constants of motion, sonic points occurred at larger distances. We showed that for correct solutions the adiabatic index of electron and proton fluid varies from non-relativistic to relativistic values. We also showed that, different cooling processes become important for different values of \dot{M} . Therefore radiative efficiency depends on \dot{M} . For $\dot{M} < 0.1$, whether it is a super massive BH or a stellar one, the accretion flow is inefficient. However for super-massive BH, the accretion flow becomes radiatively efficient i.e., more than 10% for $\dot{M} \gtrsim 0.6$. For stellar mass BH, the accretion becomes radiatively efficient when the accretion rate is close to Eddington rate. It is observed that whenever local inverse-Compton processes dominate, the accretion flow becomes luminous. Therefore, it is not necessary that radial accretion is radiatively inefficient.

References

1. Hoyle, F., and Lyttleton, R. A. 1939, Proc. Cam. Phil. Soc., 35, 405
2. Bondi, H. 1952, MNRAS, 112, 195.
3. Schmidt, M., 1963, Nature, 197, 1040
4. Bowyer, S., Byram, E. T., Chubb, T. A., Friedman, H., 1965, Science, 147, 394.
5. Salpeter, E. E., 1964, ApJ, 140, 796.
6. Michel, F. C., 1972, Ap& SS, 15, 153.
7. Shapiro, S. L., 1973, ApJ, 180, 531.
8. Shakura N. I., & Sunyaev R. A., 1973, A&A, 24, 337.
9. Liang E. P. T., Thompson K. A., 1980, ApJ, 240, L271 (LT80)
10. Fukue J., 1987, PASJ, 39, 309.
11. Nakayama K., Fukue J., 1989, PASJ, 41, 271.
12. Chakrabarti S. K., 1989, ApJ, 347, 365
13. Nakayama K., 1992, MNRAS, 259, 259.
14. Molteni D., Lanzafame G., Chakrabarti S. K., 1994, ApJ, 425, 161.
15. Lanzafame G., Molteni D., Chakrabarti D., 1998, MNRAS, 299, 799
16. Fukumura K., Tsuruta S., 2004, ApJ, 611, 964.
17. Fukumura K., Kazanas D., 2007, ApJ, 669, 85.
18. Chattopadhyay I., Chakrabarti S. K., 2011, Int. J. Mod. Phys. D, 20, 1597
19. Kumar R., Chattopadhyay I., 2013, MNRAS, 430, 386
20. Kumar R., Singh C. B., Chattopadhyay I., Chakrabarti S. K., 2013, MNRAS, 436, 2864
21. Kumar R., Chattopadhyay I., 2014, MNRAS, 443, 3444
22. Chattopadhyay I., Kumar R., 2016, MNRAS, 459, 3792
23. Kumar R., Chattopadhyay I., 2017, MNRAS, 469, 4221

24. Gu Wei-Min, Lu Ju-Fu, 2004, Chinese Physical Letters, 21, 2551
25. Chakrabarti, S. K., Molteni, D., 1995, MNRAS, 417, 672
26. Becker, P. A., Le, T., 2003, ApJ, 588, 408
27. Becker, P. A., Das, S., Le, T., 2008, ApJ, 677, L93
28. Le T., et. al., 2016, ApJ, 819, 112.
29. Lee J. P., Becker P. A., 2017, MNRAS, 465, 1409.
30. Shapiro, S. L., Lightman, A. P., & Eardley, D. M., 1976, ApJ, 204, 187
31. Shvratman, V. F., 1971, Soviet Astr. — AJ, 15, 377.
32. Colpi M., Maraschi L., Treves A., 1984, ApJ, 280, 319
33. Chakrabarti, S. K., Titarchuk, L. G., 1995, ApJ, 455, 623
34. Mandal S., Chakrabarti S. K., 2005, A&A, 434, 839
35. Laurent P., Titarchuk L., 1999, ApJ, 511, 289.
36. Narayan R., Yi I., 1995, ApJ, 452, 710
37. Nakamura K. E., Kusunose M., Matsumoto R., Kato S., 1996, PASJ, 48, 761
38. Nakamura K. E., Kusunose M., Matsumoto R., Kato S., 1997, PASJ, 49, 503
39. Manmoto T., Mineshige S., Kusunose M., 1997, ApJ, 489, 791
40. Rajesh S. R., Mukhopadhyay B., 2010, MNRAS, 402, 961
41. Dihingia I. K., Das S., Mandal S., 2017, MNRAS, 475, 2164
42. Blumenthal G. R., Mathews W. G., 1976, ApJ, 203, 714.
43. Chattopadhyay I., 2008, in Chakrabarti S. K., Majumdar A. S., eds, AIP Conf. Ser. Vol. 1053, Proc. 2nd Kolkata Conf. on Observational Evidence of Black Holes in the Universe and the Satellite Meeting on Black Holes Neutron Stars and Gamma-Ray Bursts. Am. Inst. Phys., New York, p. 353
44. Chattopadhyay I., Ryu D., 2009, ApJ, 694, 492
45. Titarchuk L., Mastichiadis A., Kulafis N. D., 1997, ApJ, 487, 834.
46. Kazanas D., Hua X.-M., Titarchuk L., 1997, ApJ, 480, 735.
47. Ipser J. P., Price R. H., 1982, ApJ, 255, 654.
48. Davies R. E., Pringle J. E., 1980, MNRAS, 191, 599.
49. Beskin G. M., Karpov S. V., 2005, A&A, 440, 223.
50. Stepney S., 1983, MNRAS, 202, 467
51. Chandrasekhar, S., 1938, An Introduction to the Study of Stellar Structure, Dover, New York.
52. Sygne J. L., 1957, The Relativistic Gas, Amsterdam, North Holland.
53. Cox J. P., Giuli R. T., 1968, Principles of Stellar Structure, Vol. 2. Gordon and Breach Science Publishers, New York
54. Vyas, M. K., Kumar, R., Mandal, S., Chattopadhyay, I., 2015, MNRAS, 453, 2992.
55. Stepney, S., & Guilbert, P. W. 1983, MNRAS, 204, 1269
56. Boldt E., Serlemitsos P., 1969, ApJ, 157, 557.
57. Jones, F. C., 1971, ApJ, 169, 503.
58. Novikov I. D., Thorne, K. S., 1973, in Dewitt B. S., Dewitt C., eds, Black Holes. Gordon and Breach, New York, p. 343.
59. Dermer C. D., Liang E. P., Canfield E., 1991, ApJ, 369, 410
60. Turolla R., Nobili L., Calvani M., 1986, ApJ, 303, 573